Supplementary Information

Title:

FDA-approved ferumoxytol displays anti-leukaemia efficacy against cells with low ferroportin levels

Authors:

Vicenta Trujillo-Alonso[†], Edwin C. Pratt[†], Hongliang Zong, Andres Lara-Martinez, Charalambos Kaittanis, Mohamed O. Rabie, Valerie Longo, Michael W. Becker, Gail J. Roboz, Jan Grimm, Monica L. Guzman

[†] *Equal contribution*
Correspondence should be addressed to M.G. at mlg2007@med.cornell.edu and J.G. at grimmj@mskcc.org

Supplementary Table 1. List of leukaemia cell lines used for in vitro studies in Figure 1A, 1B, 1E, and Figure 2. Details on morphology, type of leukaemia, mutations for each cell line and SLC40A1 expression by RTqPCR using the $2^{\Delta\Delta Ct}$ method and % positive cells by flow cytometry. ND = not determined.

Cell Line	Morphology	Type	Karyotype and/or mutation (s)	Slc40A1 2^(-ΔΔCt)/nCD34	% Ferroportin
HL60	promyelocytic	AML	c-myc+,TP53, CDK2NA/B, NRAS	0.0157	2.2
KG-1	myeloblastic	AML	OP2-FGFR1	0.5497	2.9
KCL22		CML in blast crisis	BCR-ABL	ND	4.1
UKE-1	megakaryoblastic	Essential Thrombocythemia	JAK2V617F	0.0842	4.3
MV411	monocytic	AML, M5	FLT3-ITD, MLL-AF4	0.0035	5.3
REH	Lymphoblastic	ALL (non-B, non T)		0.0187	8.2
ME-1	myeloblastic	AML, M4	INV 16 (p13;q22)	0.0036	8.3
KASUMI-1	myelomonocytic	AML, M2	AML1-ETO, N822K c-kit, TP53,CDK2NA/B	0.1421	8.6
U-937	monocytic	AML, M5	CALM-AF910	0.0408	11.1
THP-1	monocytic	AML, M5	MLL-AF9	0.0471	11.8
OCI-AML2	myeloblastic	AML, M4	NPM1 wt, DNMT3A R635W mutant	0.1726	13.5
SET-2	megakaryoblastic	Essential Thrombocythemia	JAK2V617F	3.8015	17.9
MOLM13	monocytic	AML, M5	FLT3-ITD, MLL-AF9, CDN2Adel, CDKN2B del	0.0001	22.3
K562		CML	BCR-ABL, CDKN2A del,CDKN2B del	0.1594	31.5
HEL	erythroleukemia	AML, M6	JAK2V617F, CDKN2A del, CDKN2B del	2.4425	44.9
TF-1	erythroleukemia	AML		1.8999	62.3
TUR	monocytic	AML, M5	TPA-U937 Resistant	0.0380	ND
SKM-1	monocytic	AML, M5	p53 anti-oncogene	0.0987	ND
OCI-AML3	myeloblastic	AML, M4	human hyperdiploid karyotype. NPM1 mutant	0.0978	ND
SKNO-1	myeloblastic	AML, M2	AML1-ETO, N822K c-kit	0.3001	ND
Murine Leukaemia	CML in blast crisis	ND	BCR/ABL-Nup98/HoxA9 translocation	0.03	ND

Supplementary Table 2. Primary AML samples used in Figure 3 with available de-identified information. SLC40A1 expression by RTqPCR using the $2^{\Delta\Delta Ct}$ method and % positive cells by flow cytometry ND = not determined.

ID	Sample information	Slc40A1 2^(-ΔΔCt)/nCD34		% Ferroportin		
		Blasts	CD34+	Blasts	CD34+	CD34+CD38-
AML 1	ND	0.3	ND	ND	ND	ND
AML2	M4; Normal cytogenetics; Relapsed	1.1	ND	6.5	4.4	3.4
AML3	ND	0.3	ND	43.3	26.6	34.3
AML4	De Novo; M2; Normal cytogenetics	2.1	ND	41.1	46.1	43.7
AML5	MDS progression to AML	1.2	ND	30.1	11.6	9.5
AML8	ND	3.0	ND	8.2	4.6	3.8
AML9	ND	ND	0.065	ND	ND	ND
AML10	del(9)(q13)[1]; De Novo	0.3	0.5708	ND	ND	ND
AML12	De Novo; Normal cytogenetics	0.3	ND	ND	ND	ND
AML14	MDS progression to AML	0.0	ND	57.1	57.2	59.3
AML15	Refractory; 4, XY, +8[3]	0.1	ND	ND	ND	ND
AML18	Normal cytogenetics; FLT3-ITD+, mut/NPM1; De Novo	0.2	0.1488	ND	ND	ND
AML20	FLT3-ITD+	1.7	0.0078	ND	ND	ND
AML32	ND	ND	0.1868	ND	ND	ND
AML33	ND	ND	0.2622	ND	ND	ND
AML34	NPM1 type A	ND	0.3550	60.9	ND	ND
AML37	Relapsed	0.3	1.7360	ND	ND	ND
AML52	ND	0.8	ND	ND	ND	ND
AML54	ND	0.5	1.1080	44.1	18.6	6.5
AML55	ND	0.2	ND	73	ND	ND
AML61	ND	1.0	2.2389	10.1	9.8	6.8
AML72	NPM1 type A	0.1	ND	40.8	ND	ND
AML73	ND	1.6	ND	ND	ND	ND
AML74	NPM1 type A	0.5	ND	ND	ND	ND
AML75	NPM1 type A	0.8	ND	36.4	0.97	ND
AML76	ND	0.8	ND	39.9	25.7	15.2
AML79	ND	0.1	ND	15.6	8.4	4.7
AML80	ND	ND	ND	48.3	12	29.0
AML81	ND	ND	ND	66.5	3.0	44.4
AML82	ND	ND	ND	9.9	0.0	0.0
AML83	ND	ND	ND	5.9	0.0	0.0
AML90	ND	ND	ND	4.8	1.5	1.8
AML91	FLT3 wt, NPM1 wt	ND	ND	14.6	0.0	ND
AML92	ND	ND	ND	42.5	7.9	0.0
AML93	ND	ND	ND	54.1	11.3	22.0

Supplementary Table 3. Reagent list of antibodies and dyes used for flow cytometry.

Surface Marker/Viability dye	Fluorochrome	Clone	Catalog number	Lot number	Dilution	Company
Murine CD45	PECy5	30F11	103110	B219251	0.001	BioLegend
Human CD45	APC-Cy7	2D1	368516	B224328	0.01	BioLegend
Human CD45	APCH7	2D1	560178	6118754	0.01	BD Pharmigen
Human CD34	PECy7	581	560710	7054753	0.01	BD Pharmigen
Human CD38	APC	HIT2	555462	55114	0.01	BD Pharmigen
Human Ferroportin	AF405	8G10NB	NBP2-45356	A-3-101717	0.02	Novus Biologicals
Isotype IgG2b	AF405	MCP-11	NBP2-27231	AB100711A-6-042518	0.02	Novus Biologicals
4',6-Diamidino-2-Phenylindole, Dihydrochloride (DAPI)			D1306		1 ug/ml	Thermo Fisher Scientific
7-Aminoactinomycin D (7AAD)			A1310		1 ug/ml	Thermo Fisher Scientific

Supplementary Table 4. Reagent list of Taqman probes used for quantitative RT-PCR.

Gene Name	Catalog Number
IRON	
SLC40A1	Hs00205888_m1
SLC40A1 (Murine)	Mm01254822_m1
HAMP	Hs00221783_m1
TFRC	Hs00951083_m1
FTH1	Hs01000477_g1
FTL	Hs00830226_gH
IREB2	Hs00386293_m1
Antioxidant	
NFE2L2	Hs00975961_g1
HMOX1	Hs01110250_m1
GCLC	Hs00155249_m1
GCLM	Hs00157694_m1
SQSTM1	Hs00177654_m1
NQO1	Hs02512143_s1
GSR	Hs00167317_m1
GSS	Hs00609286_m1
GPX4	Hs00989766_g1
SLC7A11	Hs00921938_m1
Inflammation	
IL1a	Hs00174092_m1
IL1b	Hs01555410_g1
IL6	Hs00174131_m1
TNFα (length = 80)	Hs00174128_m1
TNFα (length = 143)	Hs01113624_g1
Housekeeping	
ABL1	Hs01104728_m1
B2M (murine)	Mm00437762_m1
Common Reagents	
SuperScript™ IV Reverse Transcriptase	11756050
SuperScript™ VILO™ cDNA Synthesis Kit	11754050
RNase Inhibitor 40U/µl Ambion	AM2682
Oligo dt (20) Thermo Fisher Scientific	18418
Taqman gene expression master mix Applied Biosystems	4369016

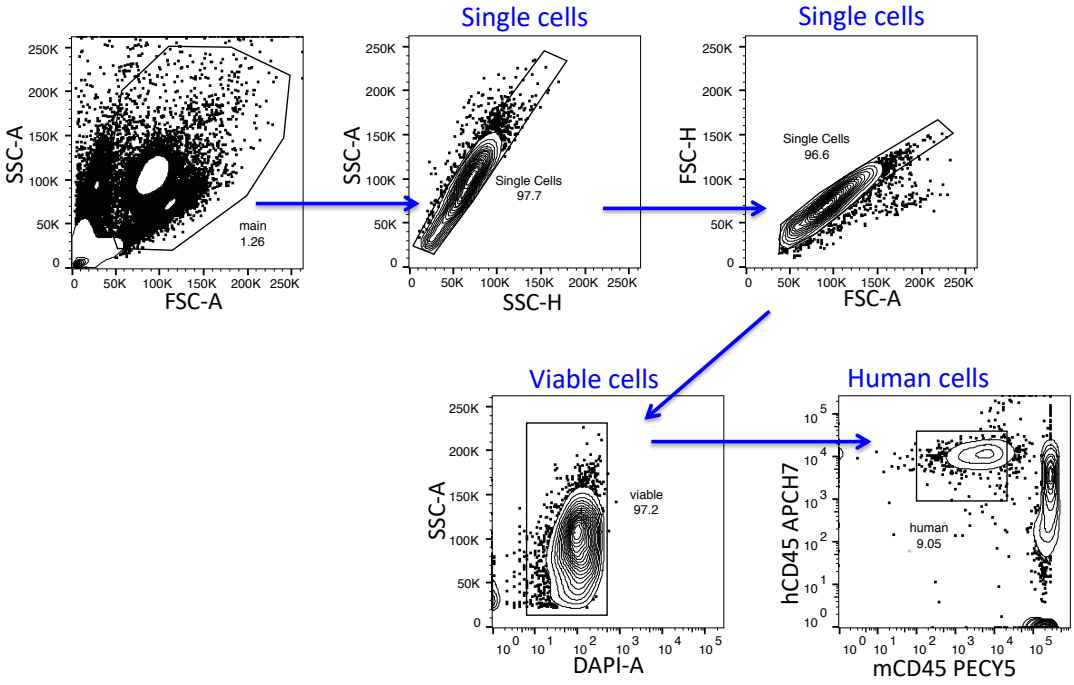

Supplementary Figure 1. Gating strategy for flow cytometry of human cells in patient derived xenografts.

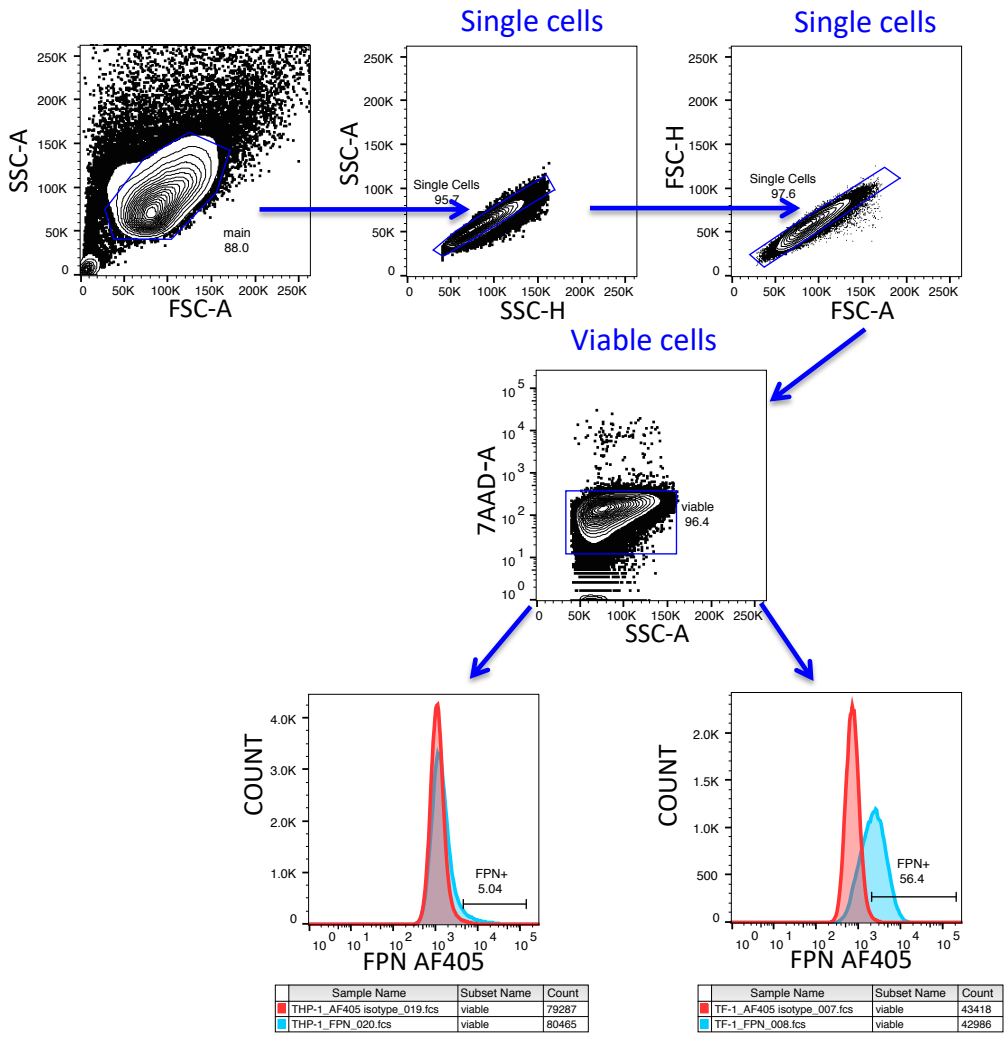

Supplementary Figure 2. Gating strategy for determination of ferroportin (FPN) in leukaemia cell lines.

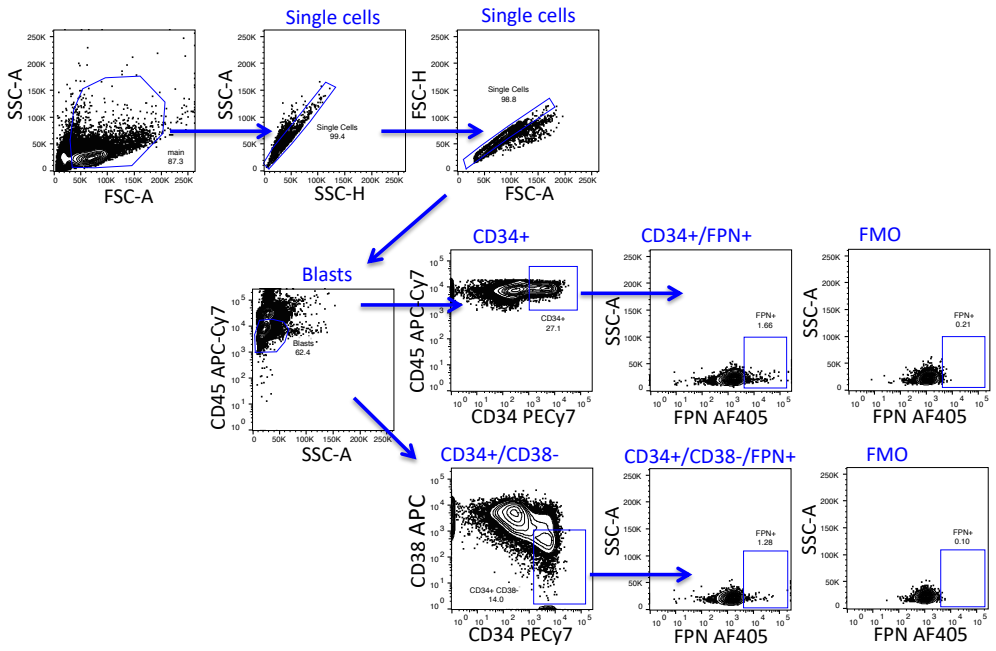

Supplementary Figure 3. Gating strategy for flow cytometry of ferroportin (FPN) expression in human primary AML samples.

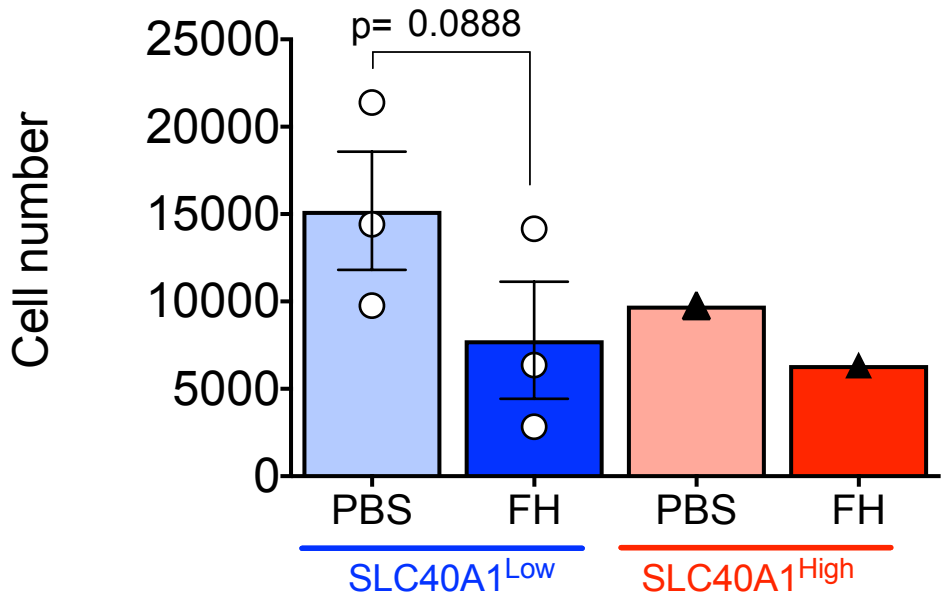

Supplementary Figure 4. Primary leukaemia sample cell survival represented by cell counts at 24h after exposure to ferumoxytol (FH) or PBS. Limited availability of primary AML high line limits biological replicates, n=3 AML patient FPN low samples/lines, n=1 patient FPN high sample. One-sided paired t-test was used for FPN Low AML lines, centre value = mean, error bars = SEM.

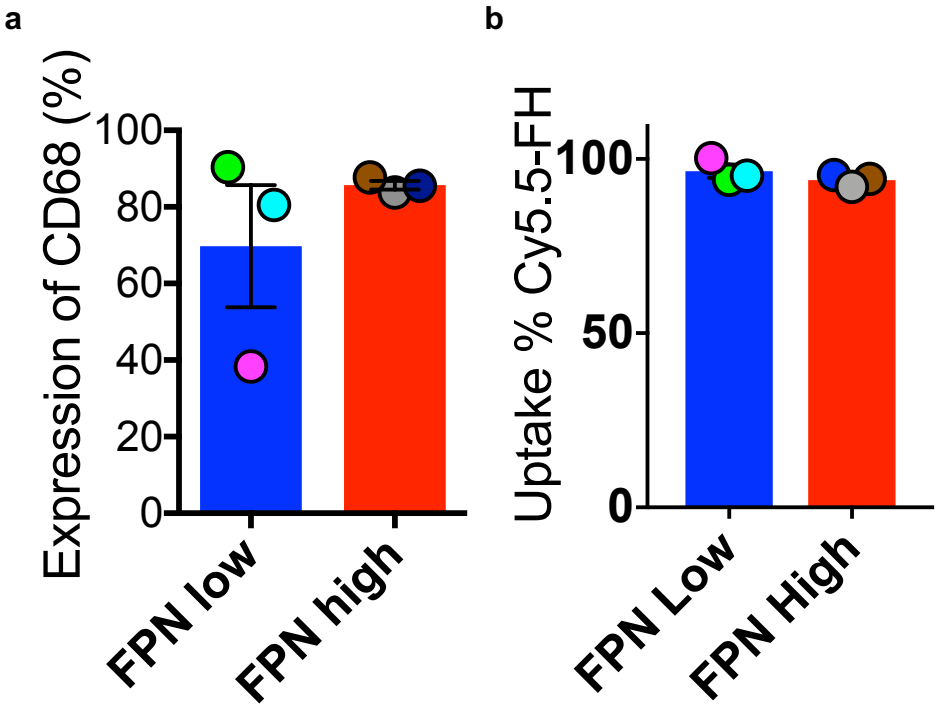

Supplementary Figure 5. CD68 expression as a marker of phagocytosis is unchanged between FPN high and low expressing lines. Similarly, Cy5.5 labelled ferumoxytol was found to be taken up across all cell lines tested. Green = KCL22, magenta = MV411, teal = UKE1, brown = SET2, grey = TF-1, navy blue = HEL. N=3 cell lines per FPN high or low group, n=2 measurements per cell line, centre value = mean, error bars = SEM.

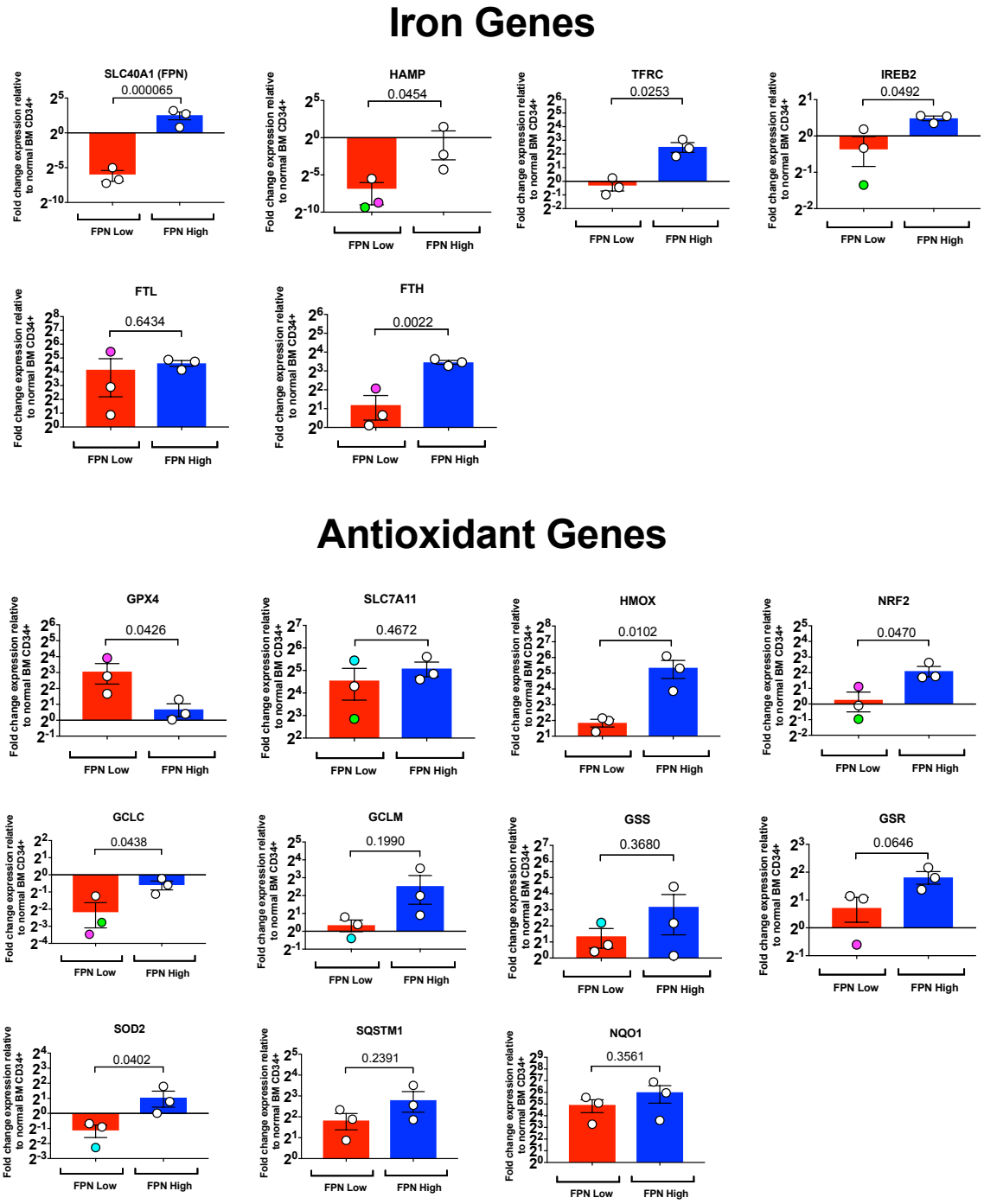

Supplementary Figure 6. mRNA expression relative of nBM stratified to FPN-low and FPN-high lines. Overall iron and antioxidant genes for FPN low cell lines are expressed at a lower level than FPN high cell lines. One clear exception for untreated FPN low cell lines is GPX4 mRNA expression showing a nearly 16-fold increase in activity relative to nBM and 4-8-fold higher than FPN high lines. Green = KCL22, magenta = MV411, teal = UKE1, brown = SET2, grey = TF-1, navy blue = HEL. N=3 cell lines per category (high or low SLC40A1), n=3 replicates per mRNA measurement, n=6 FPN low and high cell lines tested (n=3 per group), centre value = mean of cell lines, error bars = SEM on cell lines

low or high in SLC40A1. Statistics for each gene were determined using a two-tailed unpaired t-test between FPN low and high groups.

Iron Genes

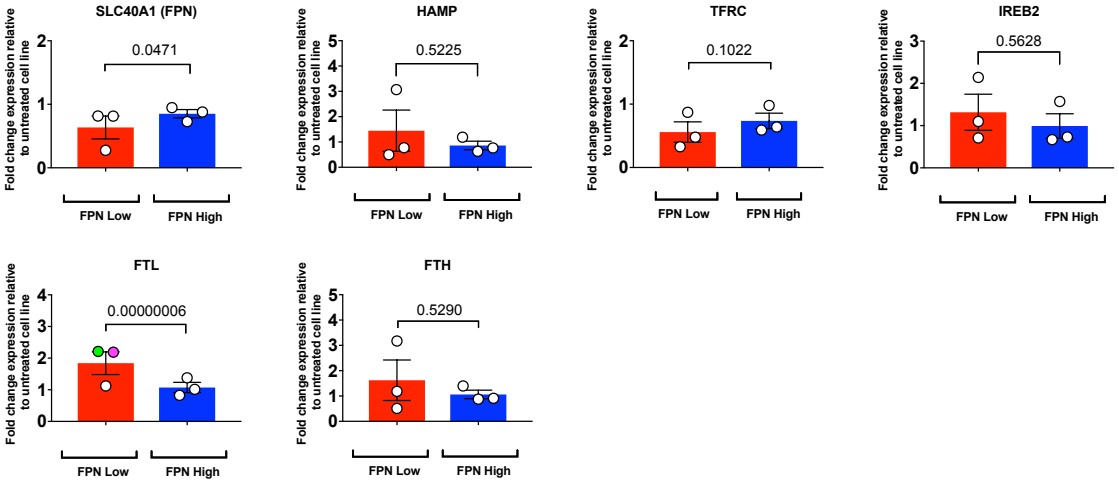

Antioxidant Genes

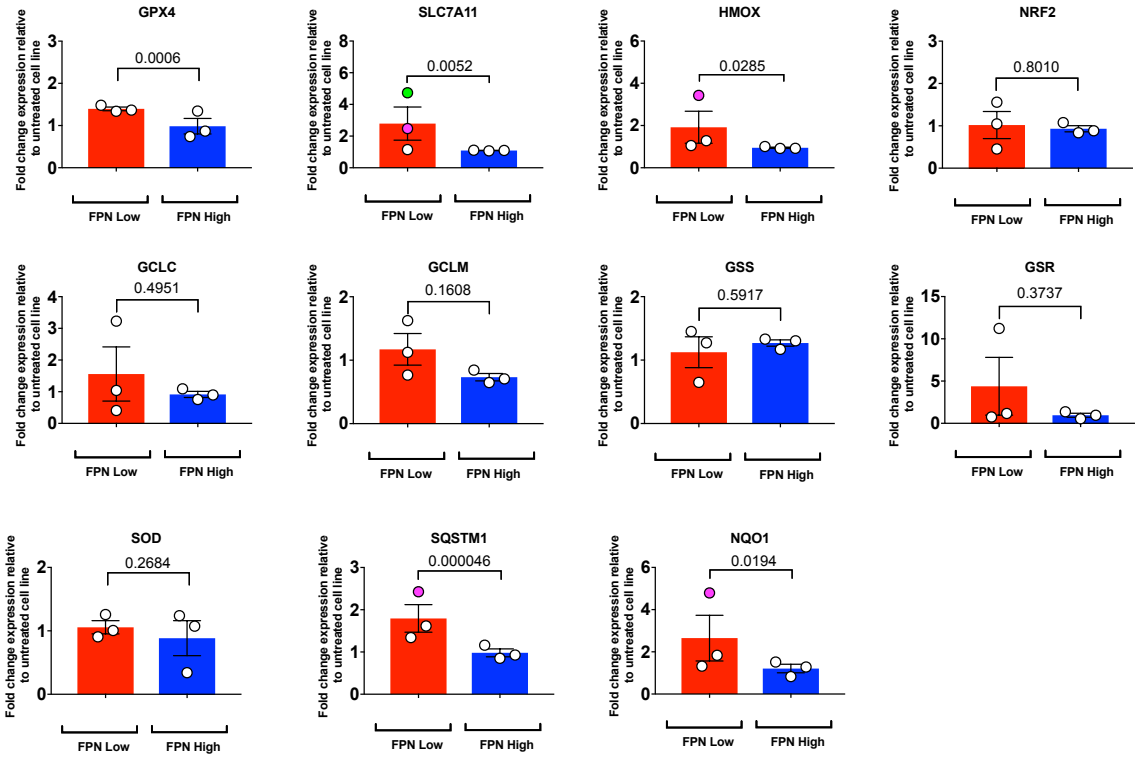

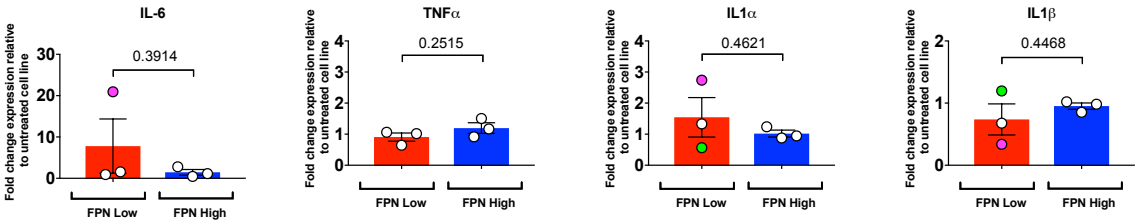

Supplementary Figure 7. Quantitative RT-PCR mRNA expression of iron, antioxidant and inflammation genes relative to untreated at 24 hours. Increases in HMOX1, SLC7A11 and FTL are the main significant changes in gene expression between ferumoxytol treated FPN low and high cell lines. Green = KCL22, magenta = MV411, teal = UKE1, brown = SET2, grey = TF-1, navy blue = HEL. N=3 cell lines per FPN low or high group, n=3 technical replicates per cell line, centre value = mean, error bars = SEM on cell lines low or high in SLC40A1. All statistics reported used two-tailed unpaired t-test.

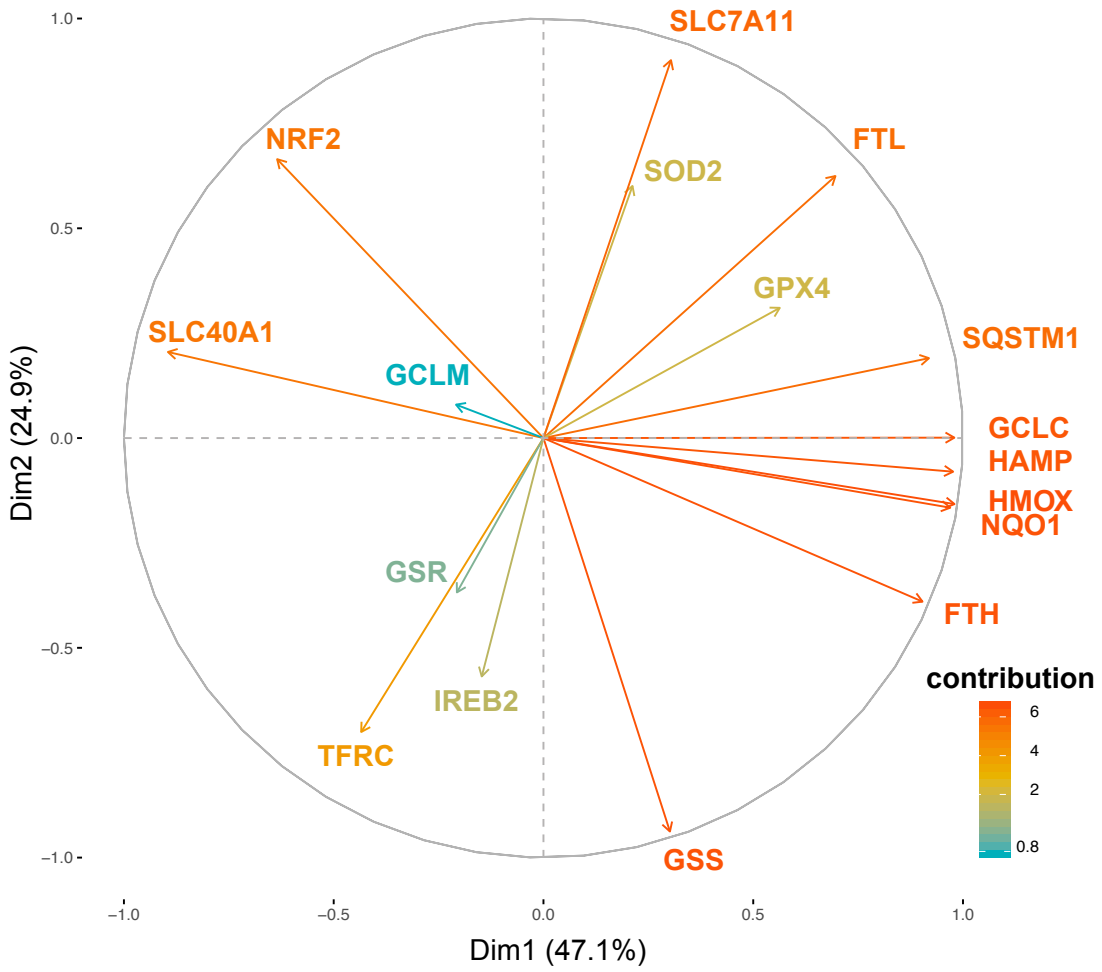

Supplementary Figure 8. Principle Component Analysis (PCA) of quantitative RT-PCR genes changes upon ferumoxytol administration relative to untreated. Largest gene cluster contains SQSTM1, GCLC, HAMP, HMOX, and NQO1 and opposes SLC40A1 (FPN) expression, meaning lower SLC40A1 expression is typically balanced by higher oxidative stress and antioxidant response genes. n=17 genes included in PCA with n=6 cell lines tested per gene with n=3 FPN low and n=3 FPN high. PCA dataset is **Supplementary Fig. 7** and values were repeated independently twice by RT-PCR before triplicate measurements were used to represent a single cell line for a specific gene. R-code was repeated four times to confirm matrix transformation and component analysis was done consistently.

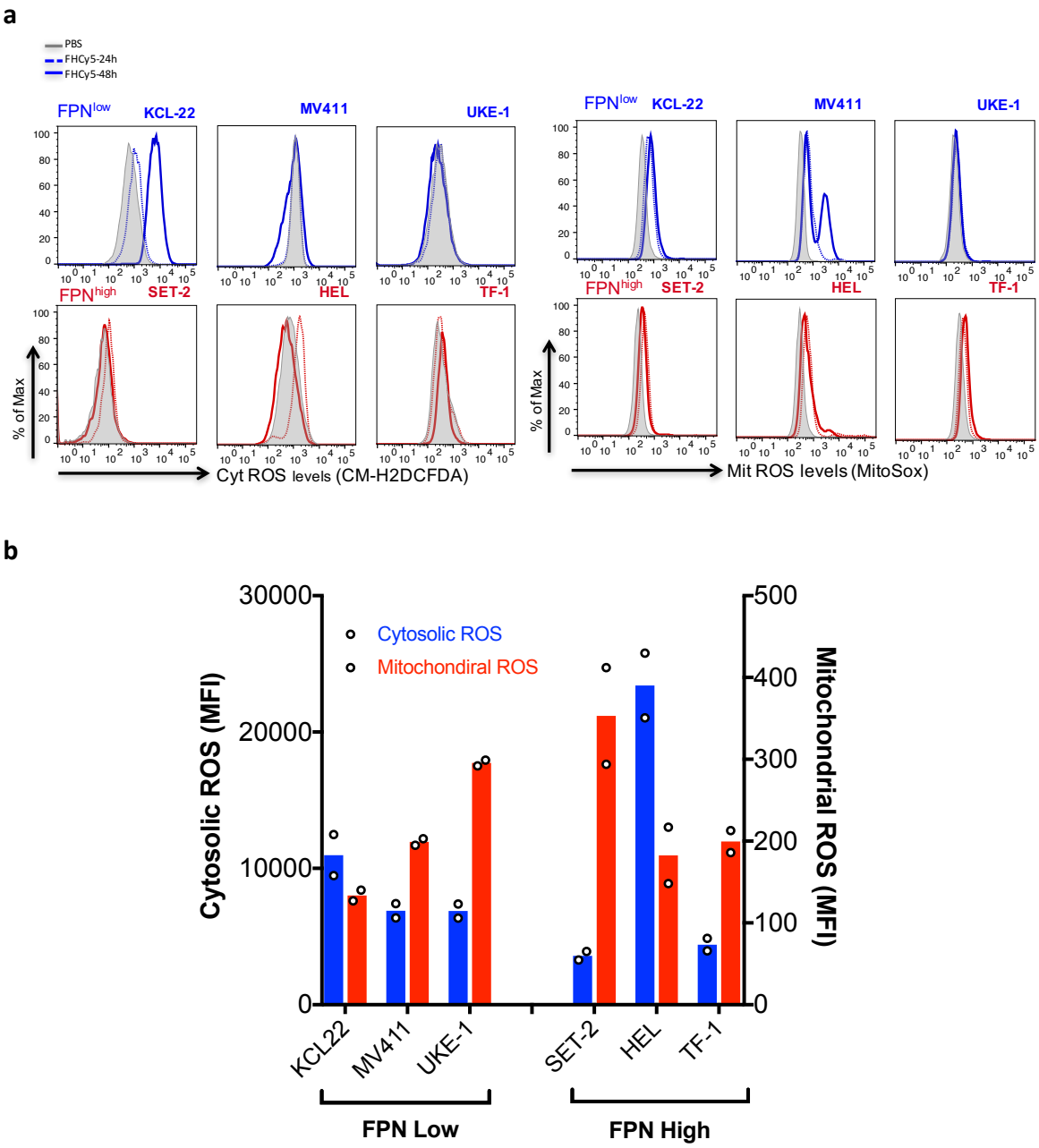

Supplementary Figure 9. Cellular and mitochondrial ROS in leukemic cell lines. A) **Fig. 1i** redrawn (n=6 cell lines n=2 technical replicates per cell line) as representative histogram from original ROS FACS scatter plot of Cy5-ferumoxytol treated AML cell lines 24 and 48 hours later showing ROS increases in FPN low (top row) lines. FPN high (bottom row) appears unchanged with ferumoxytol administration in regard to cytosolic and mitochondrial ROS production by 48 hours. B) Basal ROS levels between FPN low and high lines for cytosolic or mitochondrial ROS, n=2 technical replicates.

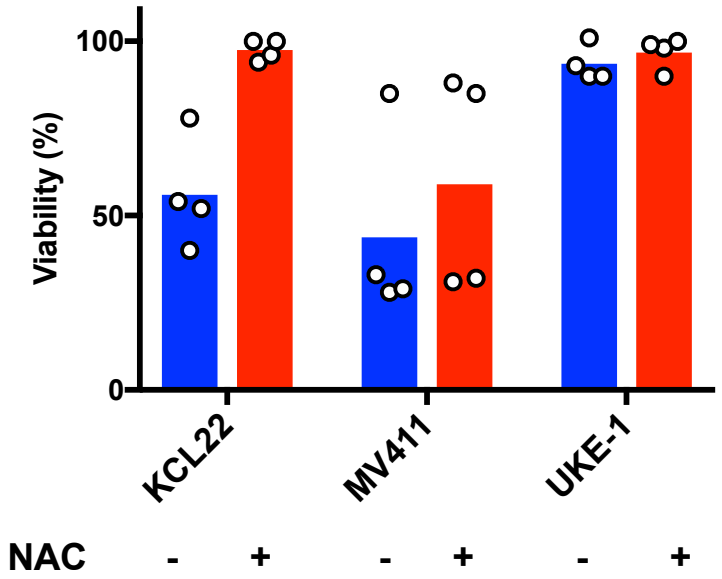

Supplementary Figure 10. Pre-treatment of FPN low expressing cell lines with N-Acetyl Cysteine (NAC) can partially protect cells from death after ferumoxytol administration. KCL22 and MV411 cell lines most sensitive to ferumoxytol administration see a full and partial protection respectively by administration of NAC. Partial protection of MV411 suggests strong ROS induction **(Supplementary Fig. 9a)** may be greater than glutathione capacity even with a supply of NAC. n=4 technical replicates per FPN low cell line, centre value = mean.

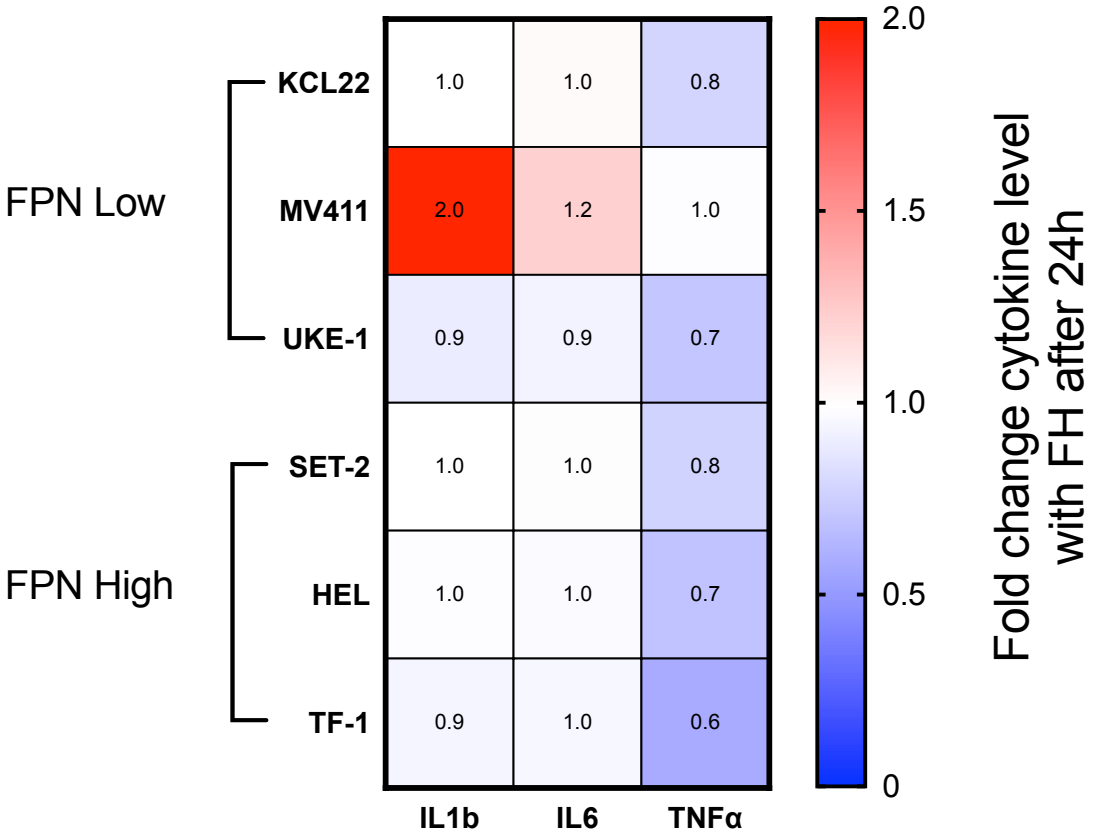

Supplementary Figure 11. Cytokine panel of AML cell lines shows no significant increase in measured cytokines upon 24h ferumoxytol (FH) exposure. Majority of measured cytokines were below the limit of detection. Heatmap normalized ferumoxytol treated to untreated lines shows no clear elevation in secreted cytokines for either FPN low or FPN high groups. N=6 biological replicates per cell line, n=8 technical replicates (IL6 TNFα), n=5 technical replicates for IL1b per cell line, value = mean fold change to untreated.

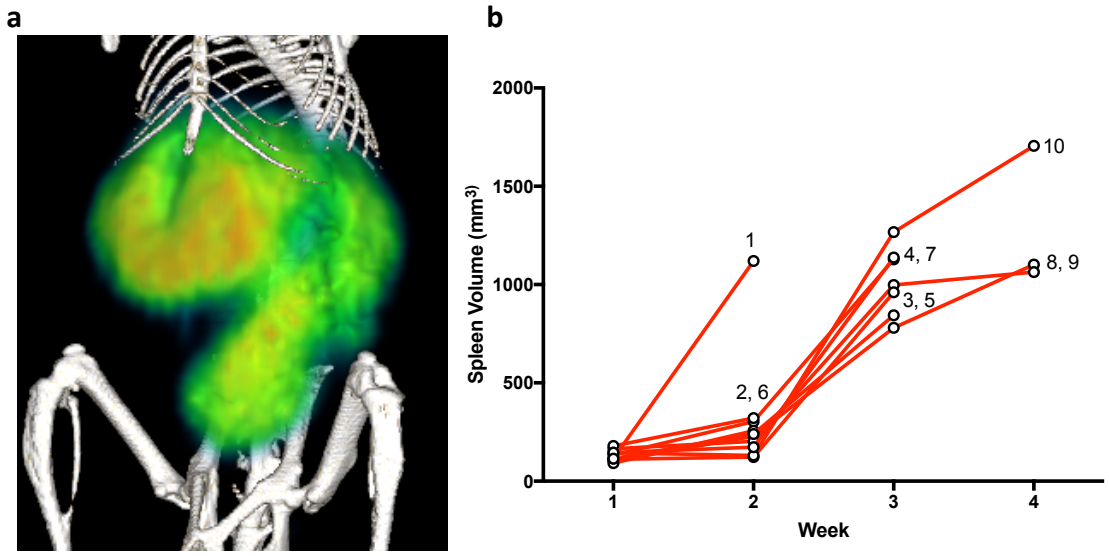

Supplementary Figure 12. ^{89}Zr-ferumoxytol PET imaging of spleen size as a function of time. A) Representative image of a mouse liver and spleen displaying splenomegaly at week 3 using ^{89}Zr-ferumoxytol 24 hours post injection. B) Spleen volumes as determined by PET region of interest shows marked spleen enlargement between 2-3 weeks. Numbers indicate order of death within cohort on Kaplan-Meier curve (**Supplementary Fig. 13**). n=10 mice per treatment group once confirmed for bcCML engraftment.

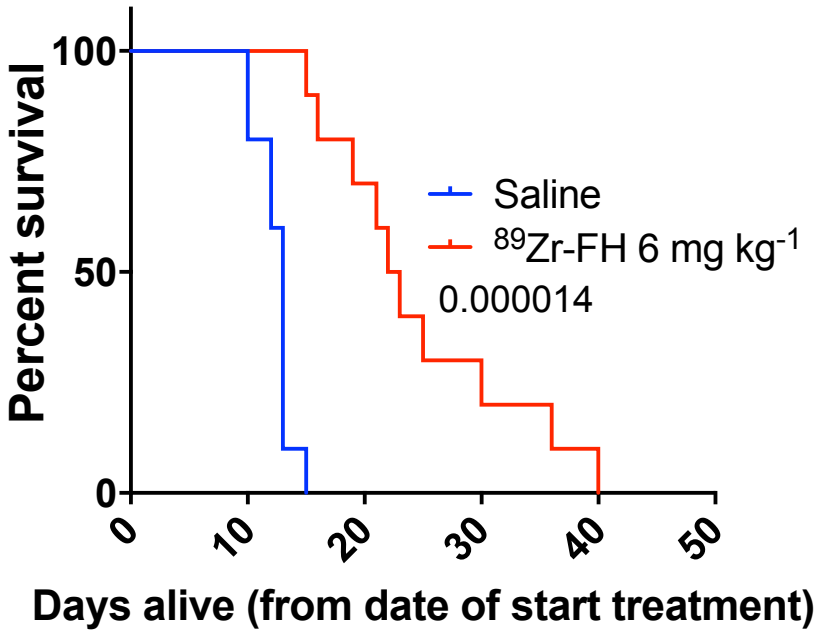

Supplementary Figure 13. Kaplan-Meier curve showing ^{89}Zr-ferumoxytol (^{89}Zr-FH) had a similar and significant survivability outcome similar to **Fig. 2i** with mice administered 6 mg kg^{-1}. Median survivability 13 days for saline, and 22.5 days for 6 mg kg^{-1} ^{89}Zr-ferumoxytol. n=10 mice per treatment group, survival curve significance determined by log-rank Mantel-Cox test.

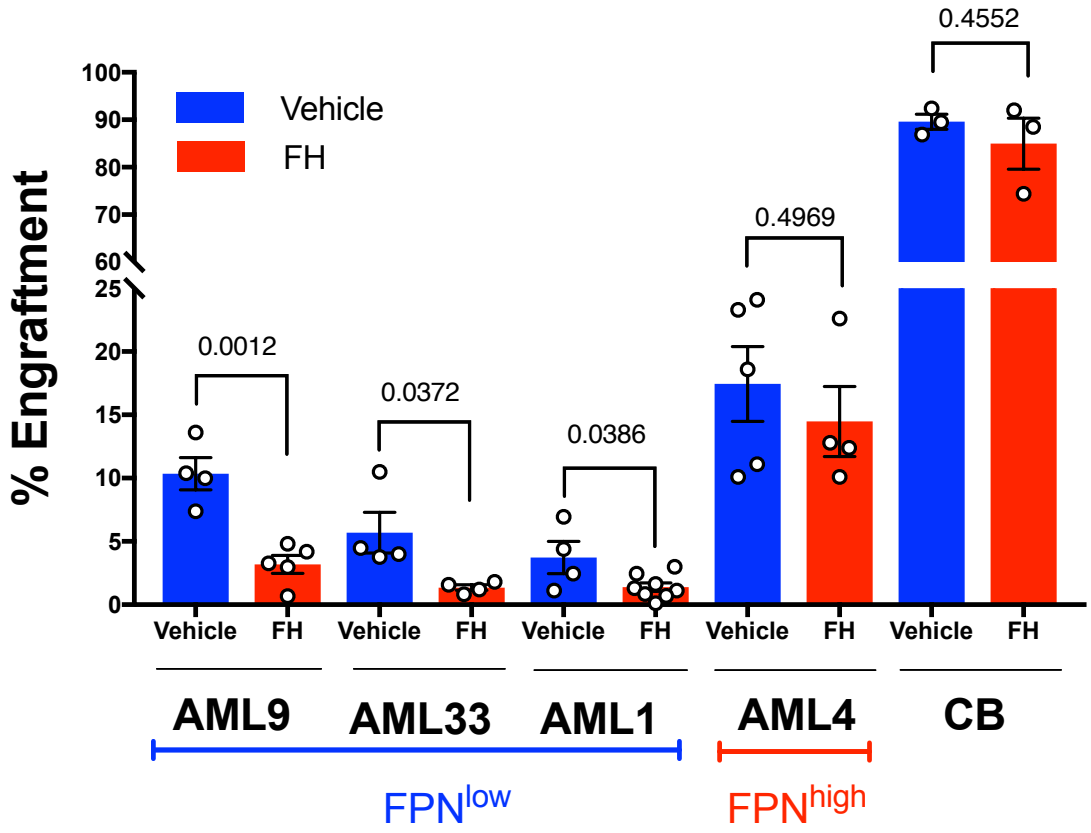

Supplementary Figure 14. Engraftment percentages for AML patient derived xenografts (AML-PDX) and CD34+ core blood. Patient derived xenografts from FPN low patients have statistically lower engraftment percentages when treated with ferumoxytol (FH). No statistical significance is seen in ferumoxytol treated FPN-high PDX sample as well as normal core blood. n=3 mice for core blood samples (Vehicle or ferumoxytol), n=4 mice for AML 9, AML 33 and AML1, n=4 for AML4 vehicle and n=8 for AML4 ferumoxytol with patient derived xenografts (vehicle or control), centre value = mean, error bars = SEM. A two-tailed unpaired t-test was used for comparison of each group between vehicle and ferumoxytol treated.

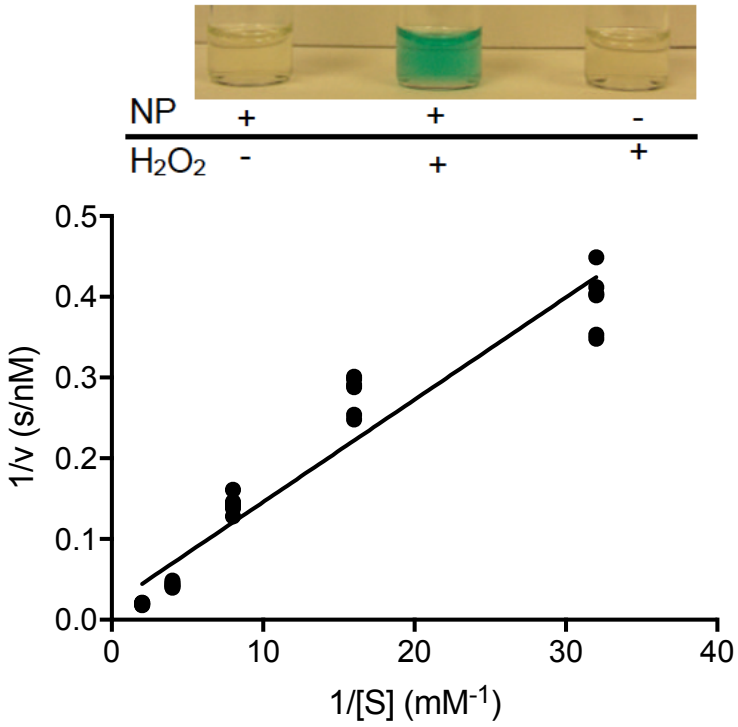

Supplementary Figure 15. Ferumoxytol has peroxidase-like activity, capable of catalyzing the conversion of organic substrates, including reporter molecules such as TMB (3,3',5,5'-Tetramethylbenzidine), in the presence of hydrogen peroxide through a Fenton-reaction-based mechanism. An increase of intracellular ROS, such as hydrogen peroxide and hydroxyl radicals as a substrate, would drive a faster rate of peroxidase activity. Peroxidase activity rates were in a manner consistent of an enzymatic or catalytic process as seen with the increase in reaction velocity with peroxide addition (n=6 technical replicates).

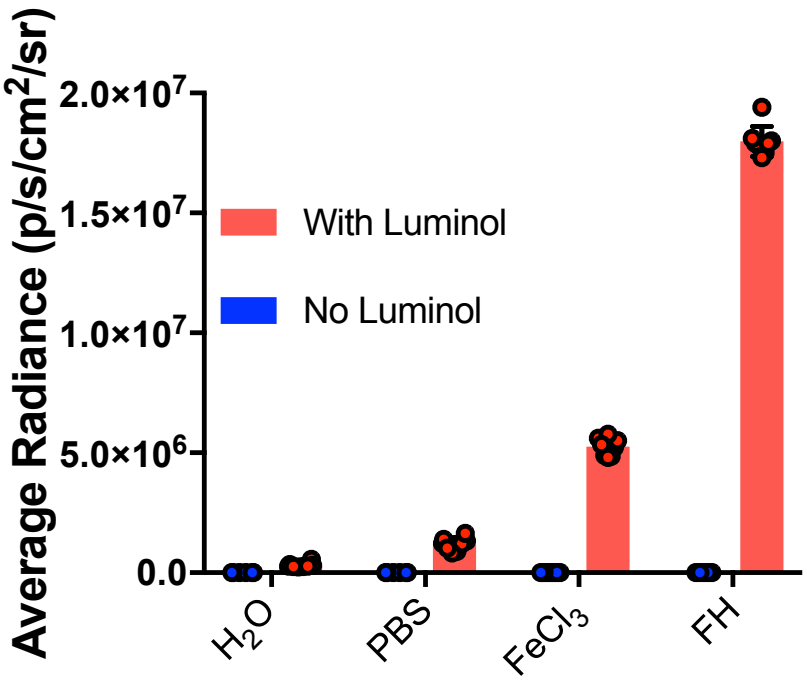

Supplementary Figure 16. Radiance measurements from luminol addition to iron sources at 1000µg Fe (n=8 technical replicates) show ferumoxytol (FH) to produce nearly 4 times the ROS as $FeCl_3$ after 30 minutes.

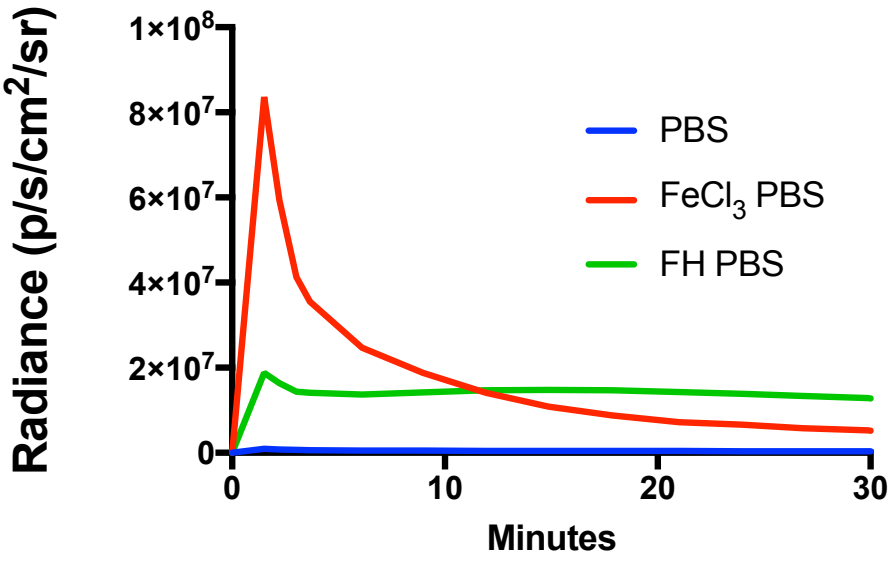

Supplementary Figure 17. Radiance measurements from the same luminol assay in **Supplementary Fig. 16** between 0-30 minutes shows a high initial ROS production followed by an exponential decrease in ROS generation with free $FeCl_3$ while ferumoxytol administration produces a nearly consistent production overtime that exceeds free $FeCl_3$ after 12 minutes. Data line plots are shown as mean, N=8 technical replicates per group.